INTERNATIONAL JOURNAL OF AUTOMOTIVE SCIENCE AND TECHNOLOGY

2025, VOL. 9, NO:1, 81-88 www.ijastech.org e-ISSN: 2587-0963

Application of Finite Elements to Analysis of Side Collision Problems of Vehicle: A Case Nissan Rogue 2020 SUV Model

Vu Hai Quan[1*], Nguyen Thanh Tung[1], Nguyen Anh Ngoc[1] and Duong Ngoc Minh[1]

[1.] *School of Mechanical and Automotive Engineering, Hanoi University of Industry, Hanoi, Vietnam*

Abstract

In this study, the authors conducted a detailed simulation of the side collision process for an SUV model using the finite element method (FEM) and Hyperworks simulation software. The specific SUV model used in this simulation was from Nissan, with various boundary conditions incorporated into the model to replicate real-world crash scenarios closely. These boundary conditions included factors such as the road surface, the collision column, the angle of impact, and the interactions between the different parts of the vehicle. For the collision speed, the authors adhered to the National Highway Traffic Safety Administration (NHTSA) standards, choosing a speed of 32km/h, which is typical for side-impact crash testing. The collision was simulated against a fixed column at an angle of 75 degrees to assess the vehicle's response. The simulation results were then evaluated based on the standards set by the Insurance Institute for Highway Safety (IIHS), specifically the guidelines outlined in their April 2024 standards. The evaluation focused on critical aspects such as the penetration of the vehicle's components at the driver's position and at the location where the car door made contact with the collision column. The results indicated that the vehicle's structure demonstrated sufficient durability, with the materials used in its construction providing adequate protection. Moreover, the penetration of various elements did not compromise the safety of the occupants, as the distance between the center of the driver's seat and the impacted door was reduced to 35.57cm, still well above the safety threshold of 18cm. This result confirms that the vehicle design meets the necessary safety standards for side-impact collisions, ensuring the protection of the driver during such an event.

Keywords: Side collision; Safe spaces; Stress; Finite element.

Research Article

History
Received 08.11.2024
Revised 19.12.2024
Accepted 16.01.2025

Contact
* Corresponding author
Vu Haiquan
quanvh@haui.edu.vn
Address: Ha Noi University of Industry, Ha Noi, Vietnam

Tel:+84981534266

To cite this paper: Quan, V.H., Tung, N.T., Minh, D.N., Ngoc, N.A. Application of Finite Elements to Analysis of Side Collision Problems of Vehicle: A Case Nissan Rogue 2020 SUV Model. International Journal of Automotive Science and Technology. 2025; 9 (1): 81-88. http://dx.doi.org/10.30939/ijastech..1581465

1. Introduction

According to the WHO “Global status report on road safety 2023”, there were approximately 1.19 million road traffic accidents worldwide in 2021 – a 5% decrease from 1.25 million accidents in 2010. More than half of the United Nations member states reduced their road traffic accidents between 2010 and 2021. The overall reduction in fatalities occurred despite a doubling of the global vehicle fleet, a significant expansion of the road network and an increase of nearly one billion people in the global population. This shows that efforts to improve road safety are working but are still far from what is needed to achieve the target of the United Nations Decade of Action on Road Safety 2021-2030 to halve road fatalities by 2030 [1].

The authors Nguyen Minh Tien et al [2] conducted a collision analysis using a car model with a dummy and an airbag in the case of a direct collision with a solid wall, one of the necessary studies on passive safety. To describe the input conditions in detail, a simulation problem on the driver's seat displacement was performed, and the data on this displacement was exported as a boundary condition for the collision simulation. The collision simulation results showed that the calculated energy values and the simulation results were almost the same (7.381e+07 and 7.367e+07); the energy was converted from kinetic energy to internal energy of the elements. The simulation results of airbag deployment were similar to the previous study by NHTSA, both in terms of graph shape and maximum value. The impact of the collision on the driver is not too great, as evidenced by the surveys of head (HIC 300), thigh (F 2.8kN), and neck (F 3.098kN; T 190Nm) injuries. However, the study conducted a deeper analysis and evaluation of the airbag structure, considering its influence on these figures, concluding that changes in the release valve size (increasing from 1000mm^2 to 2000mm^2) resulted in a decrease in the evaluated parameters. These results suggest changes to the airbag structure to improve driver safety, as well as a simpler simulation model to save analysis time.

In addition, author Shapovalenko V, with the research article "Analysis of the mechanism of side impact of cars" [3], on the side impact of two cars when participating in traffic, tends to the SUV segment and is set up so that a car that is superior to the car in terms of mass and size is a passenger car that crashes into the side. In a traffic accident with a side collision of a passenger car and an off-road vehicle in the SUV segment, the simulation shows that there is a large difference in the height of the main impact of 250mm. That is, the entire energy of the impact on the side of the passenger car does not fall on the safety bar of the SUV but is higher than 250mm, which will certainly lead to fatal injuries to the driver and passengers. Valued references to research articles on car crashes [4-9] have laid the foundation for realizing the goal of simulating side-impact crashes in terms of boundary conditions, reference results, driver safety, and safety assessment standards.

In studies on car collisions, most research has focused on frontal collisions or rollovers, adhering to standards such as ECE R64, ECE R96, or ECE R29. However, studies and simulations addressing side-impact collisions remain limited and insufficient. Based on car consumption trends in 2022 [10] and traffic accident statistics in 2023 [11], this study focuses on the SUV category and examines side-impact collisions using finite element analysis. The research employs HyperWorks software with the Radioss solver to analyze changes in vehicle components. Specifically, it evaluates the displacement of no3des and the penetration of elements from the center of the driver's seat to the impacted door panel during a collision with a pillar.

The study aims to propose and discuss detailed improvements to enhance driver safety during collisions while balancing increased costs in design and manufacturing. These improvements are aligned with safety standards outlined by the U.S. Insurance Institute for Highway Safety (IIHS) [12].

2. Theoretical Basis and Research Methodology

2.1. Finite element method

Nonlinear finite element equations of motion are often derived from the principle of virtual work. This is a weak form of the equilibrium equation that includes internal forces, contact/friction forces, inertia forces, damping forces, external forces, and boundary conditions. The finite element method (FEM) discretization of the equations of motion results in the following matrix form of the set of second-order nonlinear derivative equations:

$$[M].(\ddot{X}) + [K](X) = F_{ext} \tag{1}$$

Where (X) is the current node position vector and $(\ddot{X})$ is the node acceleration vector. [M] is the mass matrix. [K] is the stiffness matrix and F_{ext} is the vector of external forces. This equation is nonlinear (in (X) and $(\ddot{X})$) due to the presence of contacts, possible materials, and geometric nonlinearities. A time integration scheme must be chosen that is capable of dealing with this strong nonlinearity.

2.2. Calculation in vehicle collision with column

Finite element analysis is the primary method used in simulations to analyze structural strength. The energy absorbed during a collision or the deformation energy occurring in the material is calculated using the formula [13]:

$$U_e = \frac{1}{2}\int \sigma.\varepsilon.dv = \frac{1}{2}K_{eq}.\delta_{max}^2 \tag{2}$$

The specific energy absorption (SEA) parameter is evaluated to assess the material's capability to absorb energy with reduced weight, aiming to achieve improved or equivalent impact performance compared to the current structure, as described by the formula [13]:

$$SAE = U_e/\ Mass \tag{3}$$

where σ, ε and v are equal to the stress tensor; the strain tensor and the element volume respectively. Keq, an inherent property of the material, is the stiffness of the body related to the deflection (δ) and the resulting force. In elastic collisions, objects may collide with different velocities, but when they come into contact with each other, this interaction can cause them to reach the same velocity.

For inelastic collisions, objects share the same kinetic energy from the initial motion until they reach the point of maximum displacement, just before they separate [13].

$$\frac{1}{2}m_p v_p = \frac{v^2}{2}\left(m_p + m_d\right) + \frac{1}{2}K_{eq}.\delta_{max}^2 \tag{4}$$

Where m_p is the mass of the sled test, m_d is the mass of the energy absorbing tube; v_p is the velocity of the vehicle test before the collision and is the final velocity of the two masses after the collision. The initial velocity of the vehicle test is assumed to be zero.

The momentum um remains constant during the collision and is expressed by the formula [13]:

$$m_p v_p = \left(m_p + m_d\right)v \tag{5}$$

The energy conservation equation can be derived as follows:

$$\frac{1}{2}m_p v_p^2 = \frac{1}{2}m_p {v'}_p^2 + \frac{1}{2}m_d {v'}_d^2 \tag{6}$$

$$m_p v_p = m_p {v'}_p + m_d {v'}_d \tag{7}$$

Where ${v'}_p$ and ${v'}_d$ are the final velocities of the sled and energy absorbing tube from the initial state to the point of separation. The coefficient of restitution (COR) is the ratio of the difference in velocities before and after the collision [13].

$$COR = \frac{{v'}_p - {v'}_d}{v_p - v_d} \tag{8}$$

For elastic collisions, the COR value is 1.0, while for perfectly plastic collisions, the COR is 0. Plastic deformation energy is associated with the permanent failure of the component.

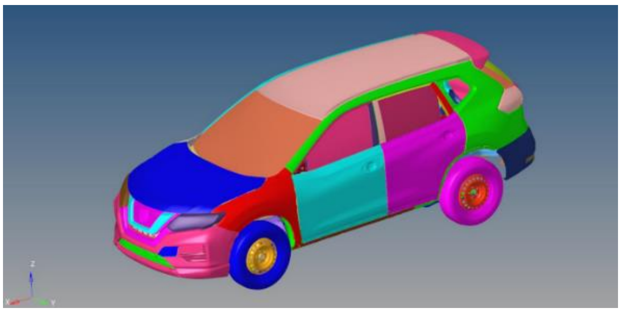

Figure 1. Nissan Rogue 2020 model.

3. Application of Finite Element Method to Formulate Lateral Collision Problems

3.1 Model setup

The study uses Hyperworks software with Radioss solver to analyze the conditions on the model; all operations are performed carefully and according to a fixed method for all cases. Thereby ensuring that all collected results have a reliable level of accuracy and contribute to the evaluation process of the results of this study. To achieve the set goals, the tasks need to be performed according to the following flow chart:

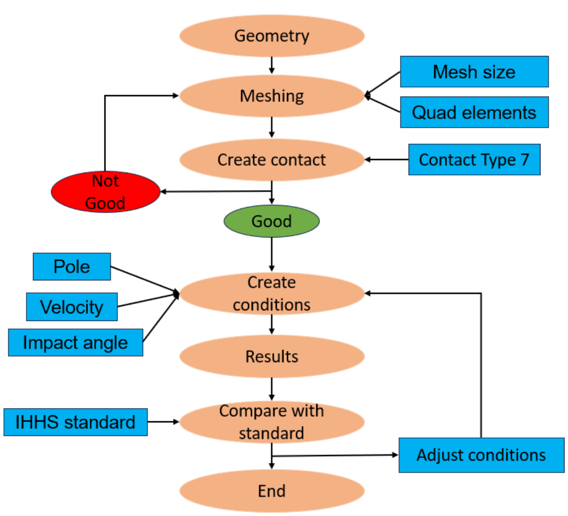

Figure 2. Steps of the process.

Based on the 3D model of the 2020 Nissan Rogue from the CCSA homepage sponsored by NHTSA, using Hypermesh software with radioss solver for meshing, the number of elements divided is 989,052 elements with mesh sizes from 6mm to 10mm.

Assign materials and their properties to the vehicle parts. The material used is steel with the specifications as shown in the table below. In addition, the properties of each vehicle part used with the image card are Pshell – sheet material, Isheel (24: QEPH shell formulation) and the thickness of each different material will be different through the setting in thickness.

Table 1. Material specifications table [14].

Parameter	Value	Unit
Rho_Initial (Density)	7.89e-9	Ton/mm^3
E (Elastic Modulus)	200000	MPa
N (Ratio)	0.3	

3.2 Set up interactions between components

Creating interactions between elements is necessary for a collision problem. This process is to create the effects of elements on each other, they will depend on each other and affect each other during the displacement process.

Set up the interaction between the parts using the TYPE7 option. The main advantage of the TYPE7 interface is that the stiffness is constant and increases as the node passes through the middle surface of the housing. This solves many problems with poor contact (common when using TYPE3 or TYPE5 interfaces) [15-16].

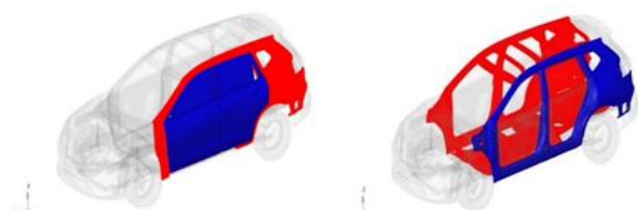

Figure 3. Interaction between the car door and other components.

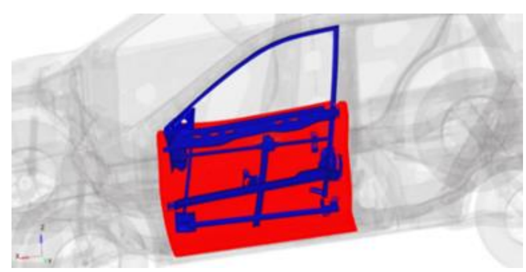

Figure 4. Interaction between the car door and chassis

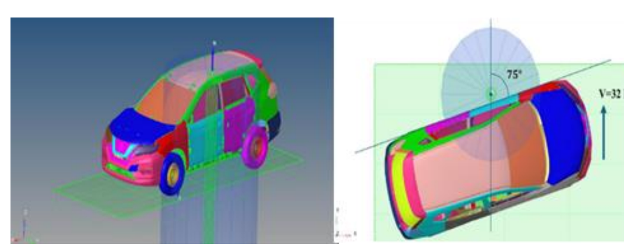

Figure 5. Road, pole, angles, and collision velocities.

Interactions are created in detail on the parts of the driver's side door because this is the collision location and the safety assessment of the structure and people in the car. In addition, the details connected together in reality are welded by the spring contact method; welding these details helps the details to be connected to each other in the simulation.

3.3 Set the road surface, column and collision velocity

Boundary conditions on velocity, road, and collision column are mandatory processes that must be performed. Establishing interactions between the vehicle and the road and column is intended to avoid the occurrence of element penetration into the road or column during a collision. Then attach the velocity to all vehicle components; the selected velocity is 32km/h based on the actual test velocity when testing vehicle collision with column, and the vehicle's tilt relative to the vertical with column is 75 degrees (according to NHTSA).

4. Results and Discussion

4.1 Car collision simulation with column.

The accuracy of the collision simulation problem is evaluated through the energy graph. After analyzing the collision with the software, the energy lines are represented as shown in the figure. The energy balance is a method to evaluate the correctness of the collision analysis. We have the total initial energy of the vehicle [17-18]:

$$E = \frac{1}{2}mv_0^2 = \frac{602.2}{2} * 8.89^2 = 23796J \approx 23796565mJ \quad (9)$$

The total energy obtained from the graph is 23781636 mJ, the difference is 1% which is acceptable.

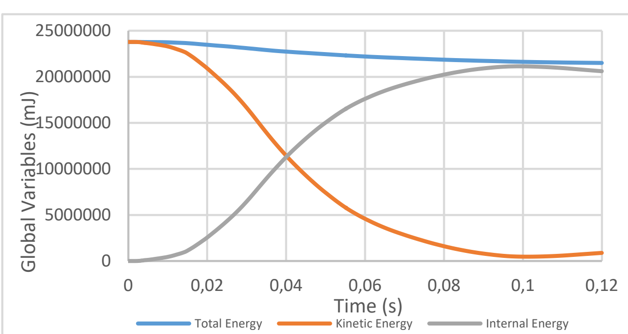

Figure 6. Energy graph.

During the collision, the total energy decreased to 21501478 mJ, the difference of 9.6% < 10% is acceptable. The energy loss is due to some interaction energy between the details in the model (Contact energy), energy error (Error energy) during the calculation process (This energy error is less than 5-10% is acceptable), so the total motion energy is reduced. The simulation result is about 90% accurate compared to the theory.

From the graph, we have the following observations:

+ Kinetic Energy remains the same from t=0s to t=0.00018s. Then the car collides with the column, causing the kinetic energy to decrease sharply to t=0.095s. From 0.095s to 0.12s, the kinetic energy changes little.

+ Internal Energy increases sharply from the start of the collision. Most of the kinetic energy is converted into internal energy, causing the deformation of the vehicle.

+ Total energy is slightly reduced. Ideally the simulation is for total energy to remain constant.

4.1.1 Vehicle durability survey

From Figure 8, it can be seen that the maximum stress is 484MPa. The details in the car door area have stress ≤ [σ] = 560MPa, which has not exceeded the steel's limit stress, thus ensuring durability.

4.1.2 Vehicle safety survey

Modern vehicles are built with safety features such as crumple zones and advanced seat belts to protect occupants from injury in the event of a collision. Unfortunately, these features do not prevent injuries when the point of impact is on the side of the vehicle. Surveying the occupant space provides initial safety assessments as well as parameters for future safety design [20].

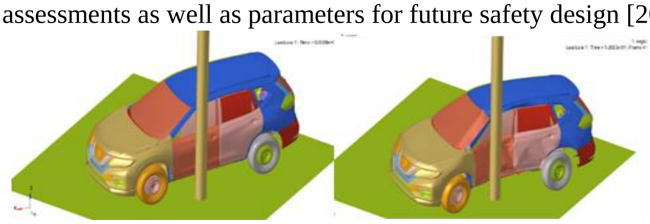

Figure 6. Cars before and after collision.

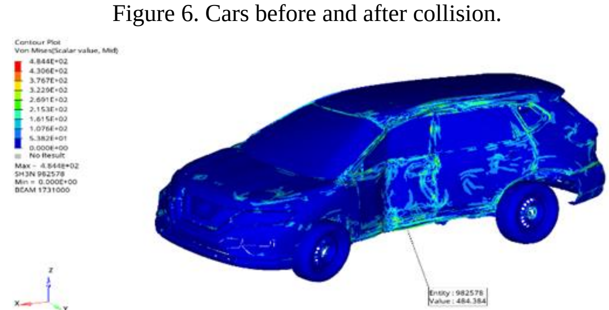

Figure 8. The stress after collision.

According to the Insurance Institute for Highway Safety (IIHS) automobile safety standards. In April 2024, the standards for analyzing car collisions with pillars were released. The safety ratings of cars are as follows:

Table 2. Material specifications.

Structural Intrusion Rating				
Infiltration	Good	Acceptable	Marginal	Least
Distance from the center axis of the vehicle frame (B-pillar) to the center of the passenger seat (cm)	≥ 18	14-17.9	10-13.9	<10

To see more clearly the degree of change between the vehicle center axis and the seat center select the node with id 2541193 representing the seat center and node 2496051 representing the most deformed part on the vehicle center axis (B-Pillar) and the distance is set in the y direction.

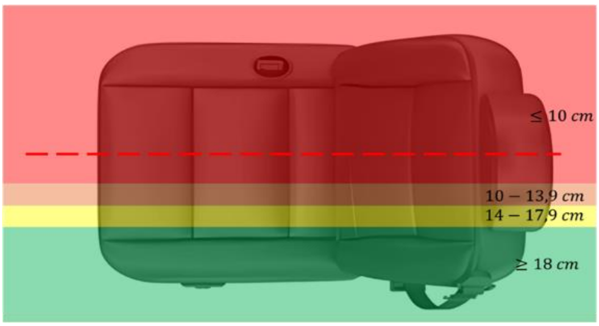

Figure 7. Safety rating according to IIHS standards.

To see more clearly the variation in distance create a cross section passing through 2 nodes.

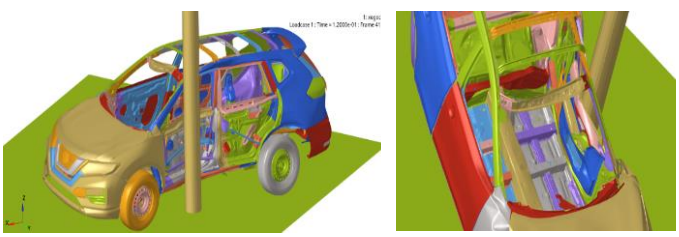

Figure 8. Car frame at time t=0.12s.

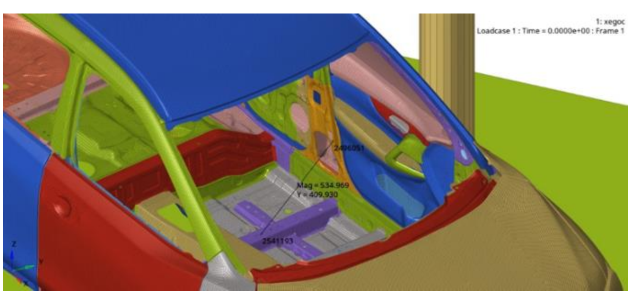

Figure 9. Two nodes selected for security evaluation.

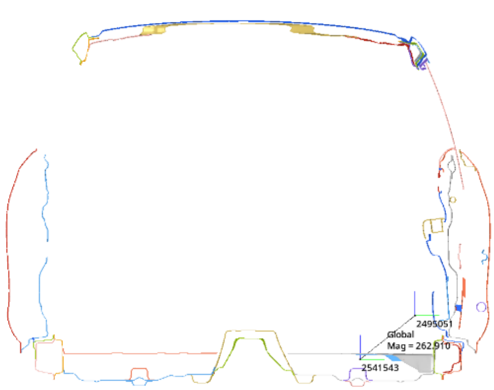

Figure 10. Distance between 2 nodes at initial time.

The distance between 2 nodes at time t= 0s is 409.930mm.

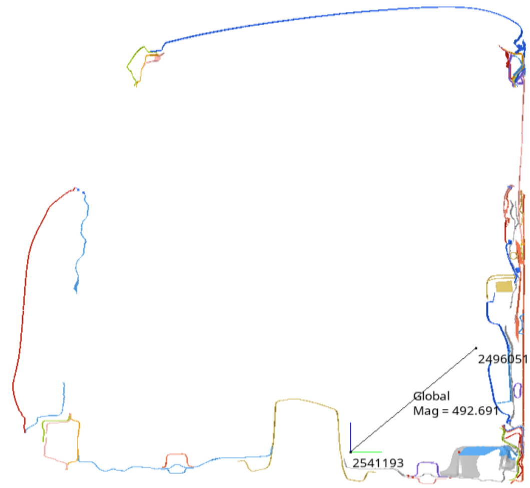

Figure 11. Distance between 2 nodes at time 0.12s.

The distance between 2 nodes at time t = 0.12s is 355.732mm, from which we can calculate the penetration as:

409.930 - 355.732 = 54.237mm

The distance from the center of the seat is:

409,930 – 54,237 = 355,693mm = 35,57cm > 18cm

It is concluded that the 2020 Nissan Rogue with the original design collided at a speed of 32km/h with a safety pillar. Compared to the IIHS standard conditions, it can be confirmed that the details ensure safety, but they are only modeling methods, so it is necessary to change the new improved cases to get the best results while still ensuring safety structure and cost.

4.2. Change 2 shock absorber bars

Based on the results obtained, a survey was conducted to investigate the case of changing the two shock absorbers to reduce the penetration of the vehicle's centerline. The shock absorbers will be drawn with additional stiffeners and replaced in the vehicle doors [21].

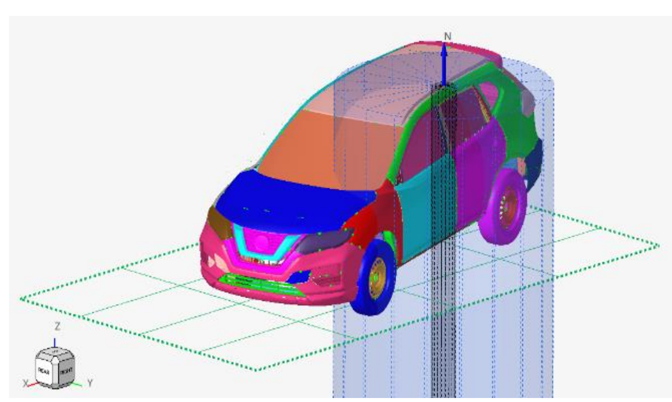

Figure 12. Replacement shock absorber bar on vehicle door

After running the simulation, the penetration measured from the distance between two nodes 2541193 and 2496051 is represented by the chart below.

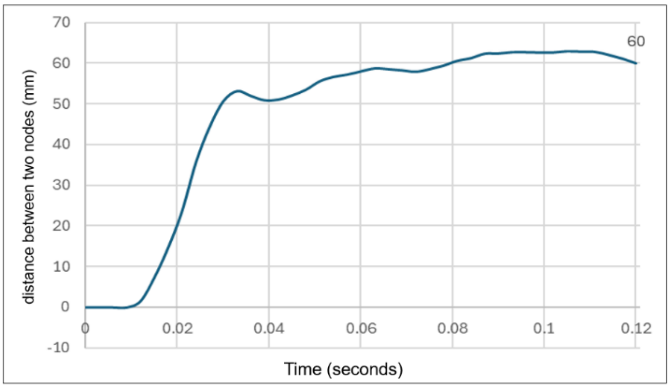

Figure 13. Penetration level between 2 nodes in case 1.

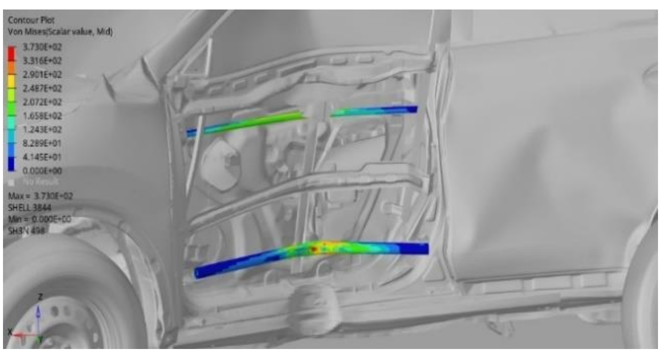

Figure 14. Stress distribution on two force-absorbing bars at time t = 0.12s.

The maximum stress on the two force-absorbing bars is 373MPa < [σ] = 560Mpa, so there is no destruction in this area.

The results obtained on the penetration of the case of changing two shock absorbers are not good. The penetration level of two nodes is still high at about 60mm, this level is not feasible, so a new alternative method needs to be selected.

4.3 Change the stiffener bar

Based on the structure, it can be seen that in a horizontal collision, the stiffener is the first bar to bear the force. Therefore, the stiffener was chosen for the survey with steel material and a thickness of 1.2mm.

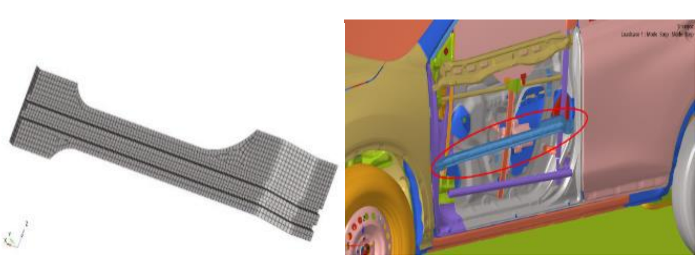

Figure 15. Replacement stiffener bar on vehicle door.

After running the simulation for case 2, the penetration measured from the distance between the two nodes 2541193 and 2496051 is represented by the chart below.

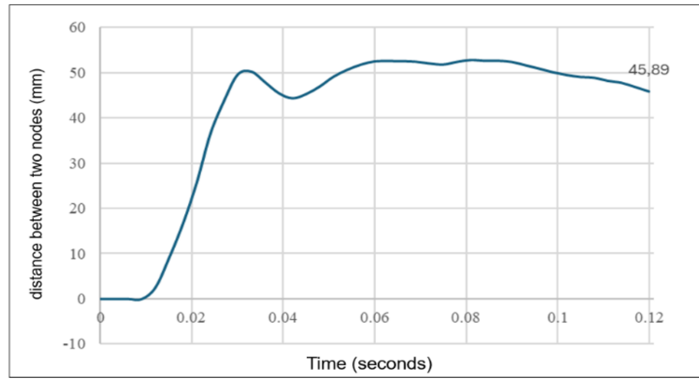

Figure 16. Penetration level between two nodes in case 2.

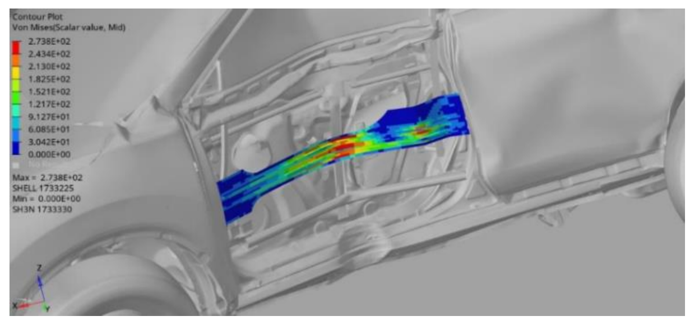

Figure 17. Stress distribution on the stiffener bar.

The maximum stress on the stiffener is 273MPa < [σ] = 560MPa, so there is no destruction in this area. The penetration level in the case of increasing the stiffener is significantly improved and feasible; the penetration is reduced to about 50 mm, thereby showing that the impact force is significantly absorbed when passing through the stiffener of the vehicle. Based on the direction of the stiffener change, perform the method of widening the stiffener to check.

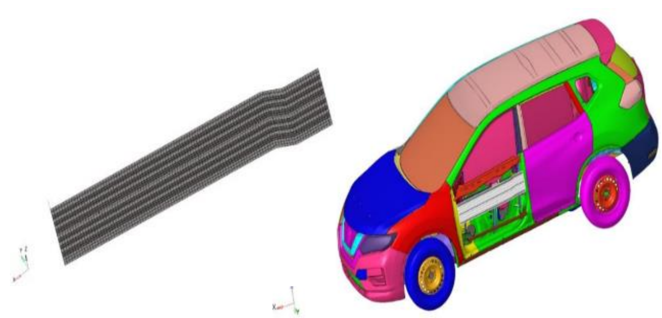

Figure 18. The stiffener bar was widened and installed on the car door.

4.4 Widen the stiffener bar

The stiffeners are increased in width while retaining the original thickness of the material. All other details of the car remain the same as the original model.

The stiffener is subjected to a large direct impact. The stress is shown in the picture and reaches its maximum at the area where the stiffener contacts the column with a stress of 274MPa < $[\sigma]$= 560MPa, so there is no destruction in this area. Although it was widened, the results obtained in case number 3 are considered not good compared to the original vehicle.

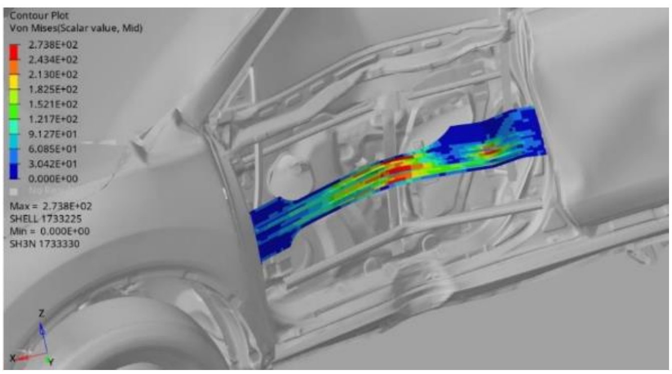

Figure 19. Stress distribution on the stiffener at time t=0.12s.

Through 3 survey cases, we obtained a graph comparing safety levels according to IIHS standards (distance from the center of the seat to the center axis of the vehicle frame).

From the graph, it can be seen that all cases have values at time 0.12s greater than 18cm, so they are considered good. In order of comparing safety, it can be affirmed that Case 2 > Initial vehicle > Case 1 > Case 3.

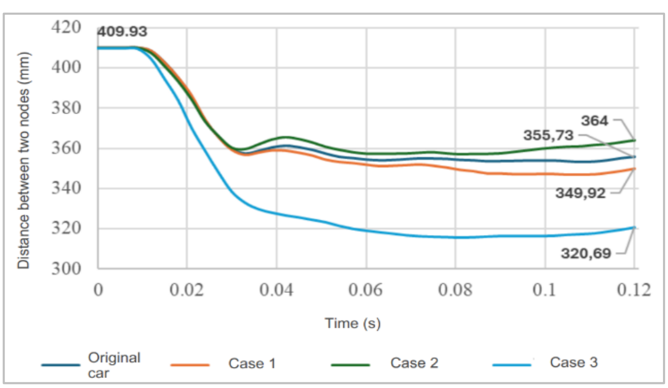

Figure 22. Penetration level between cases.

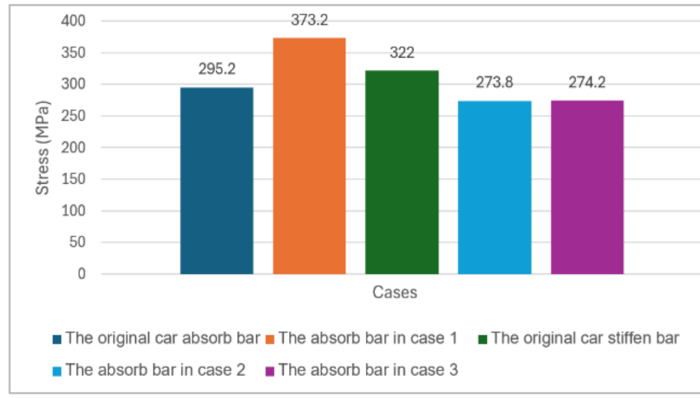

Figure 20. Maximum stress of the cases.

Table 3. Stress and intrusion table by case

Case	Initial		Change the shock absorber bar	Thicken the stiffener	Widen the stiffener bar
	Absorber bar	Reinforce ment bar			
Stress (Mpa)	295.2	322	373.2	273.8	274.2
Penetration level (mm)	355.73		349.92	364	320.69

In addition, we have a stress comparison graph in the investigated cases. It can be seen that in all cases, case 2 gives the smallest stress result and case 1 gives the largest stress result.

5. Conclusion

The study simulated a side collision with a pillar. The results showed that with the original design of the company, the safety distance for the occupants in the car was guaranteed according to the latest standards of IIHS. The results were 90% correct compared to the theory. The results obtained through 4 test cases on the 2020 Nissan Rouge showed that the original design of the car was completely safe according to IIHS collision standards. The authors investigated and expanded new cases by reinforcing additional force-absorbing details such as stiff bars or force-absorbing bars. Through those cases, it was shown that increasing the thickness of the force-absorbing bar was feasible when the stress of the detail decreased compared to the original of 48.2 MPa and at the same time the level of penetration also decreased, increasing the distance from the center of the seat to the contact position on the side of the door to 364mm wider than the original case of 8.27mm.

However, during the research process, it was only conducted at a fixed angle and fixed speed based on IIHS safety assessment standards. In order to diversify the research cases, the authors came up with the idea of implementing specific collision situations closer to reality through the results collected from this research.

Conflict of Interest Statement

The authors declared no potential conflicts of interest with respect to the research, authorship, and/or publication of this work. All authors have read and agreed to the published version of the manuscript.

CRediT Author Statement

Vu Hai Quan: Validation, writing – review and editing, writing – original draft preparation;
Nguyen Anh Ngoc: Conceptualization. Review and editing;
Nguyen Thanh Tung: Formal analysis, methodology;
Duong Ngoc Minh: Data curation, Formal analysis.

References

[1] World Health Organization. Global status report on road safety. 2015.

[2] Nguyen MT, Nguyen NA, Vu QH, Hoang DT. Identifying the influence of airbag structure on driver injury during a crash using a dummy model. EUREKA: Physics and Engineering. 2024;19(4):52-65. https://doi.org/10.21303/2461-4262.2024.003313

[3] Shapovalenko V. Analysis of the mechanism of side impact of cars. Automobile Transport. 2023;53:5-12. https://doi.org/10.30977/AT.2219-8342.2023.53.0.01

[4] Liu P. Modeling and simulation analysis of pole side impact crash test sled. International Journal of Research in Engineering and Science. 2015;3(6):1-4.

[5] Ren R, Li H, Han T, Tian C, Zhang C, Zhang J, et al. Vehicle crash simulations for safety: Introduction of connected and automated vehicles on the roadways. Accident Analysis & Prevention. 2023; 186:107021. https://doi.org/10.1016/j.aap.2023.107021

[6] Soni SS, Kumar P. Improving crashworthiness and dynamic performance of frontal plastic automotive body components. Materials Today: Proceedings. 2020; 21:1689-1695. https://doi.org/10.1016/j.matpr.2019.09.118

[7] Ly HA, Nguyen PTL, Tran DN, Nguyen TP. Reconstruction finite element model of cars. Science and Technology Development Journal of Engineering and Technology. 2021;4(1):782-789. https://doi.org/10.32508/stdjet.v4i1.782

[8] Nguyen PTL. Analysis sedan vehicle structure in frontal impact using computer model. Journal of Science and Technology. 2024;1:255-262. https://doi.org/10.53818/jfst.01.2024.255

[9] Vahedi Saheli M, Singleton PA. Injury severity analysis of rural vehicle crashes involving familiar and unfamiliar drivers. International Journal of Transportation Science and Technology. 2024;13:1-13. https://doi.org/10.1016/j.ijtst.2023.11.002

[10] Teng C, Song Z, Zhou C, Hao P, Wang B. The imperfection sensitivity of trapezoid origami crash boxes. Thin-Walled Structures. 2024; 196:111486. https://doi.org/10.1016/j.tws.2023.111486

[11] National Highway Traffic Safety Administration. Traffic Safety Facts. NHTSA's National Center for Statistics and Analysis. 2020.

[12] Quan VH, Uy DQ. Vehicle body vibration and noise impact on driver and passengers analysis: The case of the 29-seat Thaco Garden TB79s bus. Engineering, Technology & Applied Science Research. 2025; 15(1):20049-20055. https://doi.org/10.48084/etasr.9200

[13] Wen ZJ, Xu JX. Advanced lightweight materials for automobiles: A review. Materials & Design. 2022; 221:110994. https://doi.org/10.1016/j.matdes.2022.110994

[14] Guo J, Liu S, Fu Y, Liu R, Shi J. Improving the crashworthiness of B-pillars in side-collisions. Proceedings of the 7th International Conference on Mechanical, Materials and Manufacturing. 2024; 455-460. https://doi.org/10.54254/2755-2721/78/20240455

[15] Pang Y, Wong SV, Han Y, As'arry A, Ahmad Y, Tan KS. A correction method based on the simulation and experiment of side sled collision. IEEE Access. 2023; 11:3380813. https://doi.org/10.1109/ACCESS.2024.3380813

[16] Ying L, Zhang F, Dai M, Hu P. Optimization of crashworthiness for tailored hot forming B-pillar based on side impact. Journal of Mechanical Engineering. 2017; 53(12):102-108. https://doi.org/10.3901/JME.2017.12.102

[17] Purushothaman Y, Humm J, Jebaseelan D, Yoganandan N. Compression-based injury variables from chestbands in far-side impact THOR sled tests. Traffic Injury Prevention. 2019; 20(1):1-6. https://doi.org/10.1080/15389588.2019.1661681

[18] Alekhya GN, Abhishikt CBN, Ramachandran B. A recent investigation on design aspects of vehicle crash analysis in India. Materials Today: Proceedings. 2020; 27(4):3131-3136. https://doi.org/10.1016/j.matpr.2020.07.713

[19] Ziubiński M, Prochowski L. Assessment of the vehicle body side stiffness influence on the process of hazard generating in front-to-side vehicles' collision. IOP Conference Series: Materials Science and Engineering. 2024; 1247(1):012024. https://doi.org/10.1088/1757-899X/1247/1/012024

[20] Huang Z, Zhang B, Wang L, Liu C, Zhang X. Experimental study on side pole collision and deformable barrier collision of car. Journal of Physics: Conference Series. 2020; 1549(3):032120. https://doi.org/10.1088/1742-6596/1549/3/032120